Homogeneous amorphous Fe_{x}Ge_{1-x} magnetic semiconductor films with high Curie temperature and high magnetization

Yu-feng Qin, Shi-shen Yan, Shi-shou Kang, Shu-qin Xiao, Qiong Zhang, Xin-xin Yao, Tong-shuai Xu, Yu-feng Tian, You-yong Dai, Guo-lei Liu, Yan-xue Chen, Liang-mo Mei, Gang Ji, and Ze Zhang

Homogeneous amorphous Fe_xGe_{1-x} magnetic semiconductor films with high Curie temperature and high magnetization

Yu-feng Qin[1], Shi-shen Yan[1,*], Shi-shou Kang[1], Shu-qin Xiao[1], Qiong Zhang[1], Xin-xin Yao[1], Tong-shuai Xu[1], Yu-feng Tian[1], You-yong Dai[1], Guo-lei Liu[1], Yan-xue Chen[1], Liang-mo Mei[1], Gang Ji[2], and Ze Zhang[3]

[1] School of Physics, and National Key Laboratory of Crystal Materials, Shandong University, Jinan, Shandong, 250100, P. R. China

[2] Institute of Biophysics, Chinese Academy of Sciences, Beijing, 100101, P. R. China

[3] Institute of Microstructure and Property of Advanced Materials，Beijing University of Technology, Beijing, 100124, P. R. China

*Corresponding author: Shi-shen Yan

Email: shishenyan@sdu.edu.cn

Abstract：

Homogeneous amorphous Fe_xGe_{1-x} ($0.3 \leq x \leq 0.5$) ferromagnetic semiconductor films with high Fe concentration were synthesized under thermal nonequilibrium condition by magnetron co-sputtering. The microstructure, magnetism, electrical transport, and ferromagnetic resonance were systematically studied. The results indicate that Fe_xGe_{1-x} films have intrinsic ferromagnetism with high Curie temperature and magnetization. The saturation magnetization can be well fitted by Bloch's spin-wave formula in wide temperature range. Quantitative analysis of the electrical transport reveals that Fe_xGe_{1-x} ferromagnetic semiconductor films show conductivity of weakly localized carriers (holes) on the metallic side. Moreover, the anomalous Hall resistivity is proportional to the magnetization for all the samples, indicating the carriers are spin-polarized and the ferromagnetism is intrinsic. The ferromagnetic resonance further reveals that the $Fe_{0.5}Ge_{0.5}$ thin films have uniform collective ferromagnetism. Therefore, Fe_xGe_{1-x} ferromagnetic semiconductors with high Curie temperature and magnetization have potential application in spintronic devices as a high efficient spin injection source.

I. INTRODUCTION

In recent years, ferromagnetic semiconductors (FMS), which simultaneously exhibit spontaneous long-ranged ferromagnetic order and semiconducting properties, have attracted a great deal of attention due to their potential applications in spintronic devices. Compared with the well explored III-V and II-VI FMS, such as $Ga_{1-x}Mn_xAs$[1,2] and $Zn_{1-x}Co_xO$,[3] group-IV Ge-based FMS are more attractive for the compatibility with the mainstream Si-based processing technology as well as the high hole mobility. Park et $al.$[4] firstly reported that epitaxial single crystal Mn_xGe_{1-x} films showed ferromagnetism and the Curie temperature increased linearly with Mn concentration from 25 to 116K. Shuto et $al.$[5] claimed that the epitaxial $Fe_{0.175}Ge_{0.825}$ film showed an intrinsic ferromagnetism with the Curie temperature of 170K. Amorphous Ge-based FMS with high Mn concentration were also reported,[6,7] with the Curie temperature about 213K. And for co-doped $Mn_{0.13}Fe_{0.06}Ge_{0.81}$[8] and $Co_{0.12}Mn_{0.03}Ge_{0.85}$,[9] the Curie temperatures were 209K and 270K, respectively. Up to date, the main problem lies in that the Curie temperature of most Ge-based magnetic semiconductors with intrinsic ferromagnetism is below room temperature.

On the other hand, the ferromagnetism with relative high Curie temperature may occur due to the composition inhomogeneity and/or the second phases in host phase. Cho et $al.$[10,11] reported that bulk single crystal Mn, Cr, Fe doped Ge-based materials showed ferromagnetism and the highest Curie temperature was 285K, but the magnetic properties of the samples were clearly coherent with

the presence of intermetallic compounds. Goswanmi et $al.$[12] claimed that Fe-rich nanomagnets (Fe_3Ge_2) were observed in epitaxial single-crystal Ge matrix with the Curie temperature up to 230K. Jamet et $al.$[13] reported a high-T_C (>400K) ferromagnetic phase of (Ge,Mn) epitaxial layer, in which well-defined Mn-rich nanocolumns were embedded in a Mn-poor matrix. However, the ferromagnetism from the clusters or the second phases may be just local ferromagnetism, rather than the long-ranged ferromagnetism, which limits the applications of the Ge-based materials in spintronic devices.

For practical applications of the Ge-based FMS, the intrinsic ferromagnetism, high Curie temperature and spin-polarized carriers are highly desirable. Theoretical calculations predicted that Ge-based semiconductors with high Fe doping were easy to be ferromagnetic compared with Mn doping,[14] but they were less studied experimentally. Also, Paul et $al.$[15] revealed that Fe doping in MnGe led to an increase in ferromagnetic interactions as well as a decrease in the overall clustering tendency between the magnetic dopants. Therefore, further systematical study on the Fe_xGe_{1-x} magnetic semiconductor with high Fe concentration is necessary for the desirable properties.

In this paper, homogeneous amorphous Fe_xGe_{1-x} FMS films with high Fe concentrations (30-50 at %) were synthesized under thermal nonequilibrium condition by magnetron co-sputtering technology. The high Curie temperature above 350 K and the high saturation magnetization of 27.8 emu/g at 300 K were obtained in $Fe_{0.4}Ge_{0.6}$ films. The conductivity is on the metallic side of the

metal-insulator transition. Additionally, it was found that the anomalous Hall resistivity is proportional to the magnetization, indicating the carriers are spin-polarized and the ferromagnetism is intrinsic. Finally, the uniform collective ferromagnetism was confirmed by the ferromagnetic resonance.

Ⅱ. EXPERIMENTAL DETAILS

Fe_xGe_{1-x} films were synthesized on glass substrates by magnetron co-sputtering equipment with Fe (99.99%) and Ge (99.99%) targets. The thickness of all films was 300 nm. The base pressure of the chamber was better than 3.0×10^{-5} Pa, and the pressure of pure Ar (99.99%) was kept at 1.4Pa during sputtering. The growth rate of Fe was fixed at 0.2Å/s, while the growth rate of Ge varied from 0.38Å/s to 0.89Å/s. In this way, the concentration of Fe in Fe_xGe_{1-x} films can be tuned from 30 to 50 at. %. During sputtering, the substrate was rotated to ensure the uniform of the films. The glass substrate temperature was fixed at 20℃ by water cooling, which is thermal nonequilibrium growth condition for Fe_xGe_{1-x} films. The low growth temperature on the amorphous glass substrate is important to form the amorphous Fe_xGe_{1-x} phase, which greatly enhances the solubility of Fe in Ge without the impurity phases.

X-ray diffraction (XRD) with a Cu K_α radiation was used to detect the crystal structure of the films. The XRD spectra were measured from $2\theta = 20^o$ to 90° with the step size of 0.02^o. High resolution transmission electron microscope (TEM) equipped with energy dispersive x-ray spectroscopy (EDS) and selected

area electron diffraction were also used to confirm the morphology and microstructure of the films. The composition of the films was confirmed by EDS measurements. The magnetic properties were measured by superconducting quantum interference device (SQUID). We have subtracted the contribution of the substrate, which were measured after etching away the films with acid solution. Electrical transport properties, such as the conductivity and the Hall resistivity, were measured in Van der Pauw configuration by physical properties measurement system (PPMS).

III. RESULTS AND DISCUSSION

A. Structure and morphology

Figs. 1 (a)-(d) show the XRD patterns of the glass substrate and the Fe_xGe_{1-x} films. No XRD diffraction peaks were observed for all the films with different Fe concentration except the signals of amorphous glass substrate with 2θ around 25°, which indicates that the as-made films are amorphous or nanocrystal. Fig. 1(e) is the high resolution TEM image of the $Fe_{0.4}Ge_{0.6}$ film observed in the cross-section view, which evidently shows that the film is in amorphous state and the distribution of Fe atoms is uniform in nanoscale regime. Although the concentration of Fe was high up to 40 at. %, no pure Fe metal clusters or well-known Fe-Ge crystal phases were observed, which is in agreement with the results of XRD. The visible dark and bright stripes were due to the local strain, which were also observed in other experiments.[16] The amorphous structure of the

$Fe_{0.4}Ge_{0.6}$ film was also confirmed by the wide diffraction ring of the selected area electron diffraction, as shown in the inset of Fig. 1(e). In order to detect the local composition of the cross section of the samples, we used a small electron beam about 2 nm in diameter for EDS measurements. Taking $Fe_{0.4}Ge_{0.6}$ thin films as an example, the measured concentration of Fe in different regions is nearly equivalent, and the average concentration is 40.3 and 59.7 at. % for Fe and Ge, respectively. Combining the XRD and TEM results, we believe that the homogeneous amorphous Fe_xGe_{1-x} films were obtained without any detectable impurity clusters or second phases.

B. Magnetic properties

Fig. 2(a) and Fig. 2(b) show typical hysteresis loops of the $Fe_{0.5}Ge_{0.5}$ and $Fe_{0.4}Ge_{0.6}$ films measured at 30K, 150K and 300K with the applied magnetic field in the film plane. The ferromagnetism can be clearly seen from the development of coercivity and remanent magnetization in the hysteresis loops. The coercivity of $Fe_{0.4}Ge_{0.6}$ film is 7 Oe and 47 Oe at 300K and 30K, respectively. The saturation magnetization gets to $1.7\mu_B / Fe$ for $Fe_{0.5}Ge_{0.5}$ and $1.22\mu_B / Fe$ for $Fe_{0.4}Ge_{0.6}$ at 30K. It is well known that there are two equilibrium phases on the Fe-Ge phase diagram in this concentration range (30-50 Fe at. %), i.e., $FeGe_2$ and FeGe. The $FeGe_2$ is antiferromagnetic alloy and the FeGe is paramagnetic alloy, so the amorphous Fe_xGe_{1-x} ferromagnetic semiconductor is not related to the $FeGe_2$ and FeGe equilibrium phases.

Fig. 2(c) and Fig. 2(d) further show the anisotropic hysteresis loops of the $Fe_{0.5}Ge_{0.5}$ and $Fe_{0.4}Ge_{0.6}$ films measured at 30K with the magnetic field parallel and perpendicular to the film plane. For the magnetic field perpendicular to the film plane, the magnetization is hard to saturate due to the demagnetization field of the thin films. The $Fe_{0.5}Ge_{0.5}$ film shows high saturation field (the demagnetization field) due to high magnetization as compared with the $Fe_{0.4}Ge_{0.6}$ film. On the other hand, the hysteresis loops in the film plane is very easy to saturate, which show soft magnetic property with the easy magnetization plane. The obvious demagnetization anisotropy implies that the thin film forms a continuous magnetic layer rather than magnetic granular film or magnetic clusters embedded in Ge matrix. However, there is no in-plane anisotropy for all the samples with different Fe composition, which is consistent with the homogeneous amorphous state of Fe_xGe_{1-x} films. Although the magnetic anisotropy was observed in other FMS,[1] it was not reported in Ge-based ferromagnetic semiconductors.

Fig. 2(e) and Fig. 2(f) show the temperature dependence of the saturation magnetization of $Fe_{0.5}Ge_{0.5}$ and $Fe_{0.4}Ge_{0.6}$ films respectively, which was measured with 10000 Oe magnetic field in the film plane from 5K to 350K. For the $Fe_{0.5}Ge_{0.5}$ film, the saturation magnetization decreases monotonously from $1.85\,\mu_B/Fe$ to $1.45\,\mu_B/Fe$ with increasing temperature. For the $Fe_{0.4}Ge_{0.6}$ film, it monotonously changes from $1.23\,\mu_B/Fe$ to $0.65\,\mu_B/Fe$. As shown in Fig. 2 (e) and (f), both of the M-T curves can be well fitted by the Bloch's spin-wave

formula, which indicates the long-ranged ferromagnetic interaction between the Fe ions mediated by the hole carriers.[17] The well fitting is another character of good ferromagnetic semiconductors.[18,19] The Bloch's spin-wave formula used for fitting can be written as following

$$M(T) = M_0(1 - aT^{3/2}) \qquad (1),$$

where M_0 is the saturation magnetization at 0 K and a is Bloch's constant. It is clear that the experimental M-T curves are in good agreement with the formula (1) in wide temperature range from 5K to 250K for the $Fe_{0.5}Ge_{0.5}$ film and in the whole temperature range for the $Fe_{0.4}Ge_{0.6}$ film. From the experimental M-T curves, we could see that the Curie temperature is higher than 350K for these films. The fitting M_0 is $1.86 \mu_B / Fe$ for the $Fe_{0.5}Ge_{0.5}$ film and $1.24 \mu_B / Fe$ for the $Fe_{0.4}Ge_{0.6}$ film. On the other hand, the Bloch's constant a was found to decrease with increasing Fe concentration from $6.9 \times 10^{-5} \, K^{-3/2}$ for the $Fe_{0.4}Ge_{0.6}$ film to $3.2 \times 10^{-5} \, K^{-3/2}$ for the $Fe_{0.5}Ge_{0.5}$ film, which is different from the behaviour of the ferromagnetic nanoparticles.[20] This means that the spontaneous magnetization decreases more quickly with increasing temperature for low Fe concentration samples, because only the high concentration of Fe atoms can provide sufficient ferromagnetic ions and carriers to establish a robust carrier-mediated long-ranged ferromagnetism.

Fig. 3 shows the zero field cooling (ZFC) and field cooling (FC) magnetization of $Fe_{0.4}Ge_{0.6}$ film as a function of temperature with the measuring field of 50 Oe perpendicular to the film plane. After cooling the sample in zero

magnetic field from 380K to 4K, the ZFC curve was measured from 4K to 380K. As for FC measurement, the sample was first cooled from 380K to 4K with 20000 Oe magnetic field perpendicular to the film plane, and then the FC curve was obtained in a similar procedure. The ZFC and FC curves begin to overlap above 330K, a temperature much below the Curie temperature of the $Fe_{0.4}Ge_{0.6}$ film. There is no peak in ZFC curve below room temperature, which is different from the behaviour of the small ferromagnetic particles.[12,21] Supposing the cross point of ZFC and FC curves is at the blocking temperature of isolated superparamagnetic particles and the magnetic anisotropic field H_K=2500 Oe in Fig. 2 (d) is adopted, the particles' diameter should be about 42 nm, which should have been observed in XRD patterns and high resolution TEM images. Therefore, all the magnetic measurements show the uniform collective ferromagnetism, which is consistent with the homogenous Fe_xGe_{1-x} films.

C. Electric transport properties

Fig. 4 (a)-(c) show the temperature dependence of the conductivity σ_{xx} for different Fe_xGe_{1-x} films. In spite of the high concentration of Fe, the conductivity σ_{xx} smoothly decreases with temperature, which is a typical feature of semiconductor conduction. The conductivity σ_{xx} doesn't change a lot in the whole measured temperature range for all the films, indicating that the carriers are weakly localized. In doped amorphous semiconductors, on the metallic side of metal-insulator transition,[22,23] the σ_{xx}-T relation can be written by the equation

below

$$\sigma_{xx} = \sigma_0 + c_1 T^{1/2} + c_2 T \qquad (2)$$

where σ_0 is the conductivity at T = 0 K, the second term $c_1 T^{1/2}$ arises from the

Coulomb interaction of carriers in the disordered materials, and the third term

$c_2 T$ originates from the inelastic electron-phonon scattering of the weakly

localized carriers. As illustrated in Fig. 4, the experimental σ_{xx}-T curves are well

fitted by equation (2) in the low temperature range, indicating the electrical

transport behaviour on the metallic side of metal-insulator transition. Comparing

Fig.4, (a), (b) and (c), it can be found that the conductivity decreases with the

concentration of Fe for any given temperature below 300K. As the concentration

of Fe decreasing, the carriers (holes) density decreases and the localization of the

carriers dominates obviously. In this case, it is easy to understand that the fitting

parameter σ_0 decreases with the concentration of Fe, i.e., $\sigma_0 = 346 \, \Omega^{-1} \, cm^{-1}$

for $Fe_{0.5}Ge_{0.5}$ film, $\sigma_0 = 175 \, \Omega^{-1} \, cm^{-1}$ for $Fe_{0.4}Ge_{0.6}$ film, and $\sigma_0 = 135 \, \Omega^{-1} \, cm^{-1}$

for $Fe_{0.3}Ge_{0.7}$ film. On the contrary, the conductivity from the contribution of

Coulomb interaction of carriers increases with decreasing the concentration of Fe

because the Coulomb screening effect is weaker at lower carrier density.

Therefore, the fitting parameter c_1 increases with decreasing the concentration

of Fe, i.e., $c_1 = 1.57 \, \Omega^{-1} \, cm^{-1} K^{-1/2}$ for $Fe_{0.5}Ge_{0.5}$ film, $c_1 = 4.00 \, \Omega^{-1} \, cm^{-1} K^{-1/2}$ for

$Fe_{0.4}Ge_{0.6}$ film, and $c_1 = 5.62 \, \Omega^{-1} \, cm^{-1} K^{-1/2}$ for $Fe_{0.3}Ge_{0.7}$ film. We also measured

the magnetoresistance (MR) of the samples, i.e., the sheet resistivity as a function

of the magnetic field. The MR is negative and its value is very small (less than 0.1% in the field of 6 T) in the whole measured temperature range from 5 to 300 K no matter whether the applied field is parallel or perpendicular to the film plane. Usually the small negative MR is considered as a sign of moment-carrier interactions and spin polarized carriers in strongly correlated systems,[2,22,23,24,25] in contrast to small positive MR found in ordinary nonmagnetic metals[22,23] and the large positive MR observed in the disordered or inhomogeneous semiconductors.[13,26] The advantage of the small negative MR in the system of moment-carrier interactions is that the influence of the MR on the Hall effect is negligible.

The Hall Effect of the films was measured at different temperature, and the anomalous Hall Effect was dominant below the Curie temperature. The Hall resistivity is usually written by the following empirical formula,

$$\rho_{xy}(H,T) = R_0(T)\mu_0 H + R_S(H,T)M(H,T) \qquad (3),$$

where H is the external magnetic field, μ_0 is the vacuum permeability, $R_0(T)$ and $R_S(H,T)$ is the ordinary and anomalous Hall coefficients at the temperature T and the magnetic field H, respectively. Thus, the experimental Hall resistivity can be divided into two parts: the first term in equation (3) representing the ordinary Hall effect, $\rho_{xy}^o(H,T) = R_0(T)\mu_0 H$, which is proportional to H; the second term in equation (3) representing the anomalous Hall resistivity, $\rho_{xy}^a(H,T) = R_S(H,T)M(H,T)$, which is proportional to $M(H,T)$. When the external field is larger than the saturation magnetic field, the anomalous Hall

resistivity will be saturated and only the ordinary Hall Effect remains. In this case, the carriers (holes in p-type Fe_xGe_{1-x} semiconductor) density can be derived from the slope of the Hall resistivity $\rho_{xy}(H)$ in a high magnetic field region from 30000 to 60000 Oe, where the Hall resistivity $\rho_{xy}(H)$ is proportional to the magnetic field. We obtained the concentration of hole carriers is $7.3 \times 10^{21} / cm^3$ for $Fe_{0.5}Ge_{0.5}$, $5.6 \times 10^{21} / cm^3$ for $Fe_{0.4}Ge_{0.6}$, and $3.4 \times 10^{21} / cm^3$ for $Fe_{0.3}Ge_{0.7}$ films at 30K. It is clear that the hole density increases with increasing the Fe concentration. Such high hole density is responsible for the observed high Currie temperature of Fe_xGe_{1-x} magnetic semiconductor films.

The anomalous Hall resistivity ρ_{xy}^a as a function of the magnetic field (ρ_{xy}^a-H curve) for each sample at different temperature is shown in Fig. 5. The corresponding M-H curves with the same magnetic field perpendicular to the film plane at the same temperature are also illustrated in this figure. By proper scaling, we can see that the ρ_{xy}^a-H curves and M-H curves are superposed perfectly for each sample at a given temperature. Such a perfect accordance between ρ_{xy}^a-H and M-H curves indicates that single ferromagnetic ordering phase is existing,[7,25] and the observed ferromagnetism is intrinsic. We believe that the high Fe concentration in our films provides high concentration of holes and localized spins of Fe. Therefore, the intrinsic ferromagnetism should originate from the ferromagnetic exchange coupling between strongly localized spins of Fe 3d electrons, which was mediated by the weakly localized s, p holes due to the Fe partially replacing Ge sites. The strong anomalous Hall Effect with obvious

hysteresis indicates that the carriers are polarized.[1,2,4,25]

The relationship between $\rho_{xy}^a(H,T)$ and $M(H,T)$ is further shown in Fig. 6 for all the data in Fig. 5. It was found that the experimental anomalous Hall resistivity $\rho_{xy}^a(H,T)$ is proportional to the magnetization $M(H,T)$ for all the samples at any given magnetic field and temperature below the Curie temperature. This means that for each Fe_xGe_{1-x} film the slope (the value of $R_S(H,T)$) is a constant within the error of the experiments, which does not depend on the external magnetic field and temperature.

D. Ferromagnetic resonance

In order to further check the ferromagnetism and its uniformity of the Fe_xGe_{1-x} magnetic semiconductor thin films, the ferromagnetic resonance was done on some samples. Fig.7 shows the derivative spectra of the ferromagnetic resonance of the $Fe_{0.5}Ge_{0.5}$ thin film which were measured at room temperature with the frequency of 9.77 GHz. When the applied magnetic field was in the film plane, as shown in the inset (a) in Fig. 7, only one uniform resonance peak with strong intensity and narrow width was found, which is consistent with the uniform magnetization of the amorphous ferromagnetic thin film. If there exists the second magnetic phase in the $Fe_{0.5}Ge_{0.5}$ thin film, additional resonance peak should be detected. When the applied magnetic field was perpendicular to the film plane, several subsidiary peaks below the uniform resonance peak were observed, as shown in Fig. 7 and its inset (b). In the case of perpendicular

magnetic field, the separation between the subsidiary resonance field and the uniform resonance field is about 95, 392, 844, 1408, 2078, and 4800 Oe, respectively. The ratio of the separation is about $1^2:2^2:3^2:4^2:5^2:7^2$. When the angle between the external field and the film normal increases, all the resonance fields gradually decrease and finally all the subsidiary peaks except the uniform resonance peak disappear at the angle larger than 25 degree. According to the spin-wave theory of the magnetic thin films,[27] the separation between the resonance field of the nth spin-wave mode and the uniform resonance mode is proportional to n^2. The observed n^2 law in the $Fe_{0.5}Ge_{0.5}$ thin film means that the subsidiary peaks below the uniform resonance peak are spin-wave modes. A series of spin-wave modes companying a strong and narrow uniform resonance mode reveal that the $Fe_{0.5}Ge_{0.5}$ thin film has uniform collective ferromagnetism.

IV. CONCLUSIONS

In conclusion, homogeneous amorphous Fe_xGe_{1-x} ferromagnetic semiconductor films with high Fe concentration were synthesized. The Curie temperature is higher than 350K. Quantitative analysis of the electrical transport reveals that Fe_xGe_{1-x} ferromagnetic semiconductor films show conductivity of weakly localized carriers (holes) on the metallic side. Moreover, the anomalous Hall resistivity is proportional to the magnetization for all the films, indicating the carriers are spin-polarized and the ferromagnetism is intrinsic. The ferromagnetic resonance further reveals that the Fe_xGe_{1-x} thin films have uniform

collective ferromagnetism. The Fe_xGe_{1-x} ferromagnetic semiconductor with high Curie temperature and magnetization may have application in spintronic devices as a high efficient spin injection source.

ACKNOWLEDGEMENTS

References:

[1] H. Ohno, A. Sher, F. Matsukura, A. Oiwa, A. Eudo, S. Katsumoto, and Y. Iye, Appl. Phys. Lett. **69**, 363 (1996).

[2] H. Ohno, Science **281**, 951 (1998).

[3] G. L. Liu, Q. Cao, J. X. Deng, P. F. Xing, Y. F. Tian, Y. X. Chen, S. S. Yan, and L. M. Mei, Appl. Phys. Lett. **90**, 052504 (2007).

[4] Y. D. Park, A. T. Hanbicki, S. C. Erwin, C. S. Hellberg, J. M. Sullivan, J. E. Mattson, T. F. Ambrose, A. Wilson, G. Spanos, and B. T. Jonker, Science **295**, 651 (2002).

[5] Y. Shuto, M. Tanaka, and S. Sugahara, J. Appl. Phys. **99**, 08D516 (2006).

[6] Y. X. Chen, S. S. Yan, Y. Fang, Y. F. Tian, S. Q. Xiao, G. L. Liu, Y. H. Liu, and L. M. Mei, Appl. Phys. Lett. **90**, 052508 (2007).

[7] S. Yada, S. Sugahara, and M. Tanaka, Appl. Phys. Lett. **93**, 193108 (2008).

[8] R. R. Gareev, Yu. V. Bugoslavsky, R. Schreiber, A. Paul, M. Sperl, and M. Döppe, Appl. Phys. Lett. **88**, 222508 (2006).

[9] F. Tsui, L. He, L. Ma, A. Tkachuk, Y. S. Chu, K. Nakajima, and T. Chikyow, Phys. Rev. Lett. **91**, 177203 (2003).

[10] S. Cho, S. Choi, S. C. Hong, Y. Kim, J. B. Ketterson, B.-J. Kim, Y. C. Kim, and J. H. Jung, Phys. Rev. B **66**, 033303 (2002).

[11] S. Choi, S. C. Hong, S. Cho, Y. Kim, J. B. Ketterson, C. Jung, K. Rhie, B. J. Kim, and Y. C. Kim, J. Appl. Phys. **93**, 7670 (2003).

[12] R. Goswami, G. Kioseoglou, A. T. Hanbicki, O. M. J. van't Erve, B. T. Jonker,

and G. Spanos, Appl. Phys. Lett. **86**, 032509 (2005).

[13] M. Jamet, A. Barski, T. Devillers, V. Poydenot, R. Dujardin, P. Bayle-Guillemaud, J. Rothman, E. Bellet-Amalric, A. Marty, J. Cibert, R. Mattana, and S. Tatarenko, Nat. Mater. **5**, 653 (2006).

[14] H. Weng and J. Dong, Phys. Rev. B **71**, 035201 (2005).

[15] A. Paul and B. Sanyal, Phys. Rev. B **79**, 214438 (2009).

[16] J. H. Yao, S. C. Li, M. D. Lan, and T. S. Chin, Appl. Phys. Lett. **94**, 072507 (2009).

[17] Y. Fukuma, H. Asada, S. Miyawaki, T. Koyanagi, S. Senba, K. Goto, and H. Sato, Appl. Phys. Lett. **93**, 252505 (2008).

[18] J. C. A. Huang, H. S. Hsu, Y. M. Hu, C. H. Lee, Y. H. Huang, and M. Z. Lin, Appl. Phys. Lett. **85**, 3815 (2004).

[19] S. J. Potashnik, K. C. Ku, R. Mahendiran, S. H. Chun, R. F. Wang, N. Samarth, and P. Schiffer, Phys. Rev. B **66**, 012408 (2002).

[20] A. Franco1, V. S. Zapf, V. B. Barbeta, and R. F. Jardim, J. Appl. Phys. **107**, 073904 (2010).

[21] S. Gangopadhyay, G. C. Hadjipanayis, B. Dale, C. M. Sorensen, K. J. Klabunde, V. Papaefthymiou, and A. Kostikas, Phys. Rev. B **45**, 9778 (1992).

[22] F. Hellman, M. Q. Tran, A. E. Gebala, E. M. Wilcox, and R. C. Dynes, Phys. Rev. Lett. **77**, 4652 (1996).

[23] W. Teizer, F. Hellman, and R. C. Dynes, Solid State Commun. 114, 81 (2000).

[24] L. Zeng , J. X. Cao, E. Helgren, J. Karel, E. Arenholz, Lu Ouyang, David J.

Smith, R. Q. Wu, and F. Hellman, Phys. Rev. B **82**, 165202 (2010).

[25] Y. Fukuma, M. Arifuku, H. Asada, and T. Koyanagi, J. Appl. Phys. **91**, 7502 (2002).

[26] A. P. Li, J. F. Wendelken, J. Shen, L. C. Feldman, J. R. Thompson, and H. H. Weitering, Phys. Rev. B **72**, 195205 (2005).

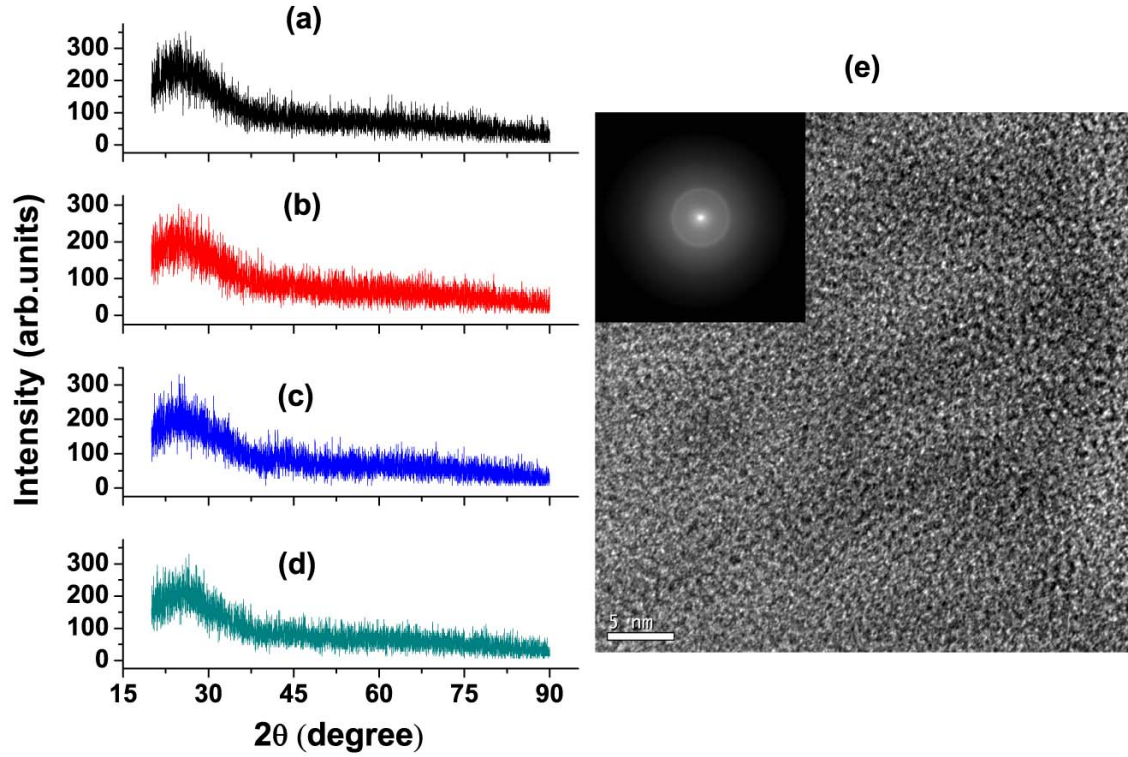[27] C. Kittel, Phys. Rev. **110**, 1295 (1958).

Figures and captions:

Fig. 1 (a) The XRD patterns of the glass substrate. (b), (c) and (d) the XRD patterns of the Fe_xGe_{1-x} films with Fe concentration 50%, 40% and 30%, respectively. (e) High resolution TEM image of the $Fe_{0.4}Ge_{0.60}$ film observed in the cross-section view. The scale bar is 5 nanometres. The inset of (e) is a selected area electron diffraction pattern of the $Fe_{0.4}Ge_{0.6}$ film.
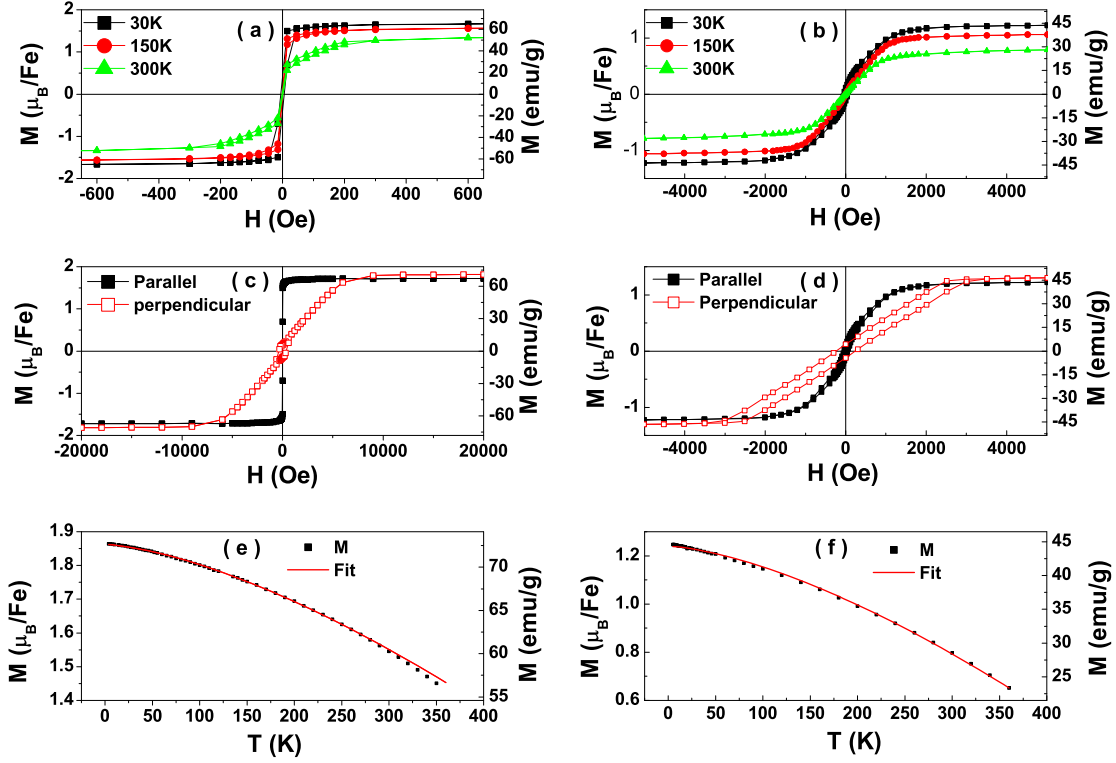
Fig. 2 (a), (b) the hysteresis loops of the $Fe_{0.5}Ge_{0.5}$ and $Fe_{0.4}Ge_{0.6}$ films respectively, which are measured with the applied magnetic field parallel to the film plane at the temperature of 30K, 150K and 300K. (c) , (d) the anisotropic hysteresis loops measured with the applied magnetic field parallel and perpendicular to the film plane at 30K for $Fe_{0.5}Ge_{0.5}$ and $Fe_{0.4}Ge_{0.6}$ films, respectively. (e), (f) the temperature dependence of the saturation magnetization measured with 10000 Oe magnetic field parallel to the film plane of $Fe_{0.5}Ge_{0.5}$ and $Fe_{0.4}Ge_{0.6}$ films, respectively. The solid lines of (e) and (f) show the fitting by formula (1) with $M_0 = 1.86\,\mu_B\,/\,Fe$, $a = 3.2 \times 10^{-5}\,K^{-\frac{3}{2}}$ for $Fe_{0.5}Ge_{0.5}$ film, and $M_0 = 1.24\,\mu_B\,/\,Fe$, $a = 6.9 \times 10^{-5}\,K^{-\frac{3}{2}}$ for $Fe_{0.4}Ge_{0.6}$ film.
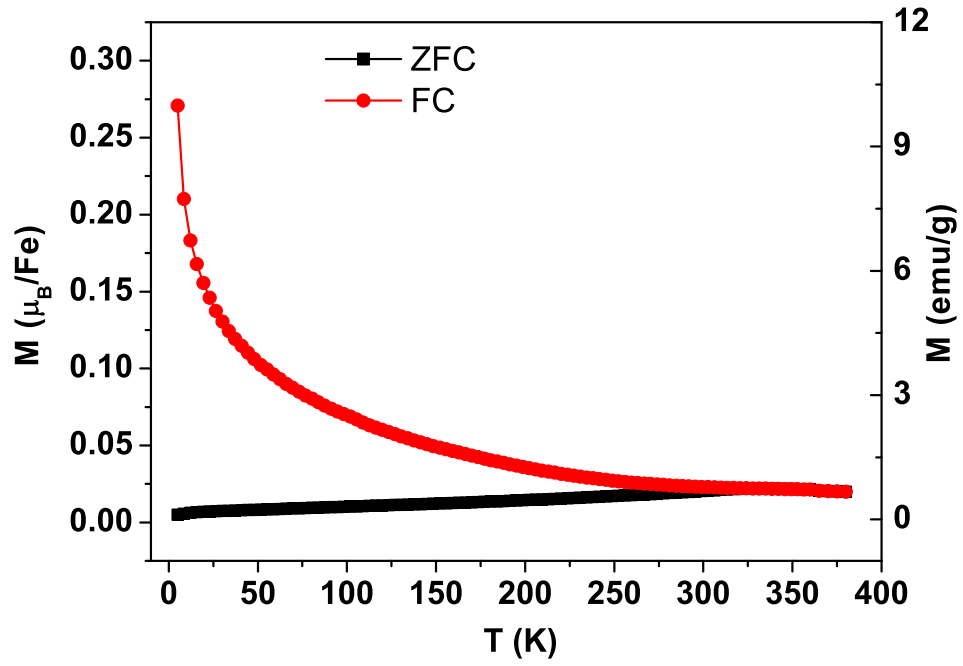
Fig. 3 The temperature dependence of ZFC and FC magnetization of the Fe$_{0.4}$Ge$_{0.6}$ film. The external magnetic field of 50 Oe was perpendicular to the film plane during the measurements. The ZFC and FC curves overlap above 330K.
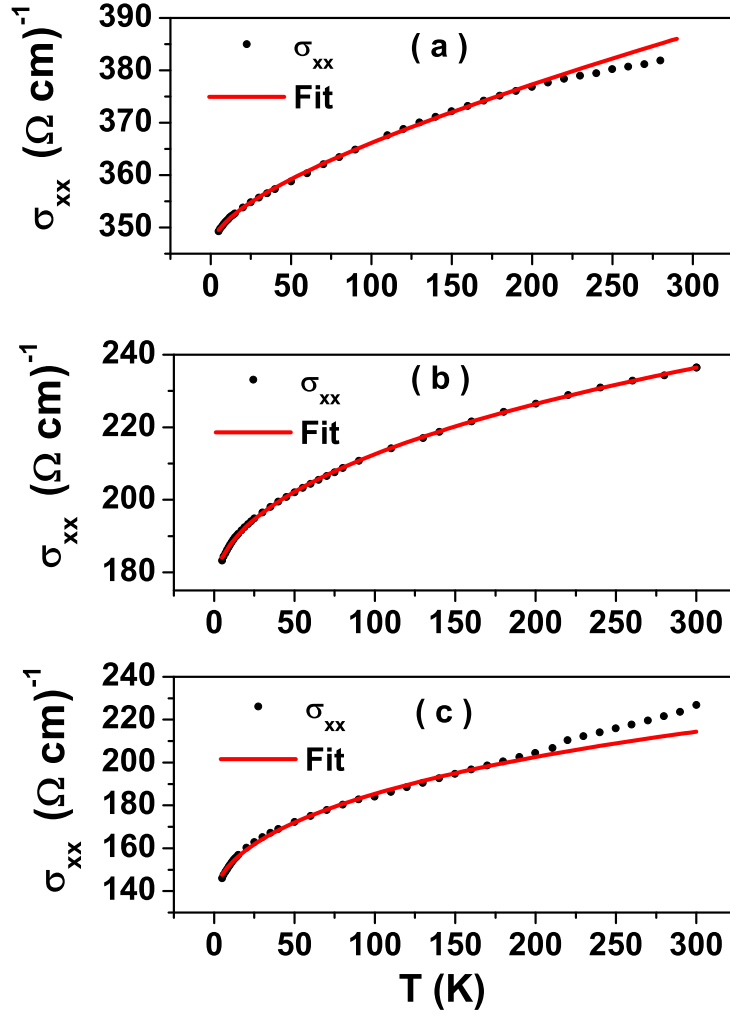
Fig. 4 The temperature dependence of the conductivity σ_{xx} of different compositional films. The solid lines in the figures show the fitting by equation (2). (a) For $Fe_{0.5}Ge_{0.5}$ film, the fitting is good from 5K to 200K with $\sigma_0 = 346\,\Omega^{-1}\,cm^{-1}$, $c_1 = 1.57\,\Omega^{-1}\,cm^{-1}K^{-1/2}$ and $c_2 = 0.047\,\Omega^{-1}\,cm^{-1}\,K^{-1}$. (b) For $Fe_{0.4}Ge_{0.6}$ film, the fitting is good from 5K to 300K with $\sigma_0 = 175\,\Omega^{-1}\,cm^{-1}$, $c_1 = 4.00\,\Omega^{-1}\,cm^{-1}K^{-1/2}$, and $c_2 = -0.03\,\Omega^{-1}\,cm^{-1}\,K^{-1}$. (c) For $Fe_{0.3}Ge_{0.7}$ film, the fitting is good from 5K to 200K with $\sigma_0 = 135\,\Omega^{-1}\,cm^{-1}$, $c_1 = 5.62\,\Omega^{-1}\,cm^{-1}K^{-1/2}$, and $c_2 = -0.06\,\Omega^{-1}\,cm^{-1}\,K^{-1}$.

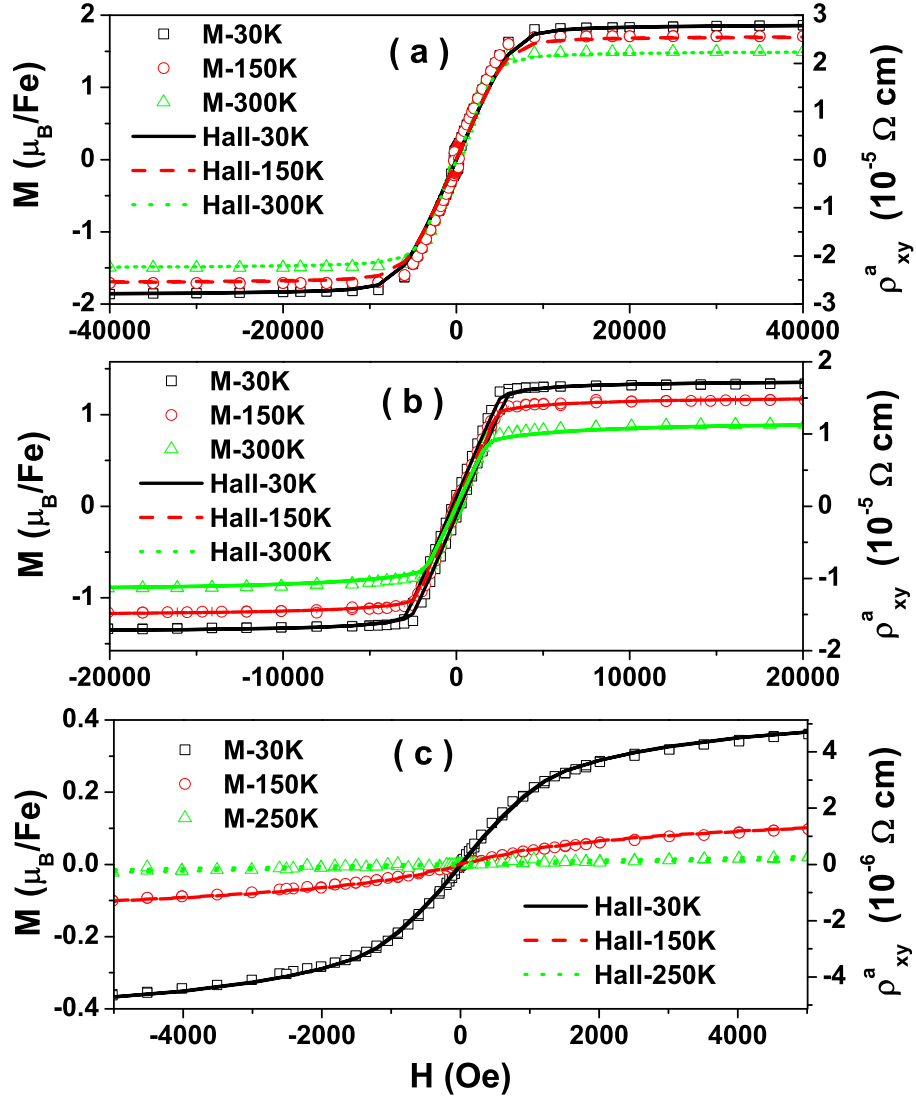**Fig. 5** M-H hysteresis loops and the corresponding anomalous Hall resistivity ρ_{xy}^a-H loops of (a) $Fe_{0.5}Ge_{0.5}$, (b) $Fe_{0.4}Ge_{0.6}$, and (c) $Fe_{0.3}Ge_{0.7}$ films. The measuring temperature is showed in the figures. The scatters represent magnetization and the lines represent anomalous Hall resistivity.
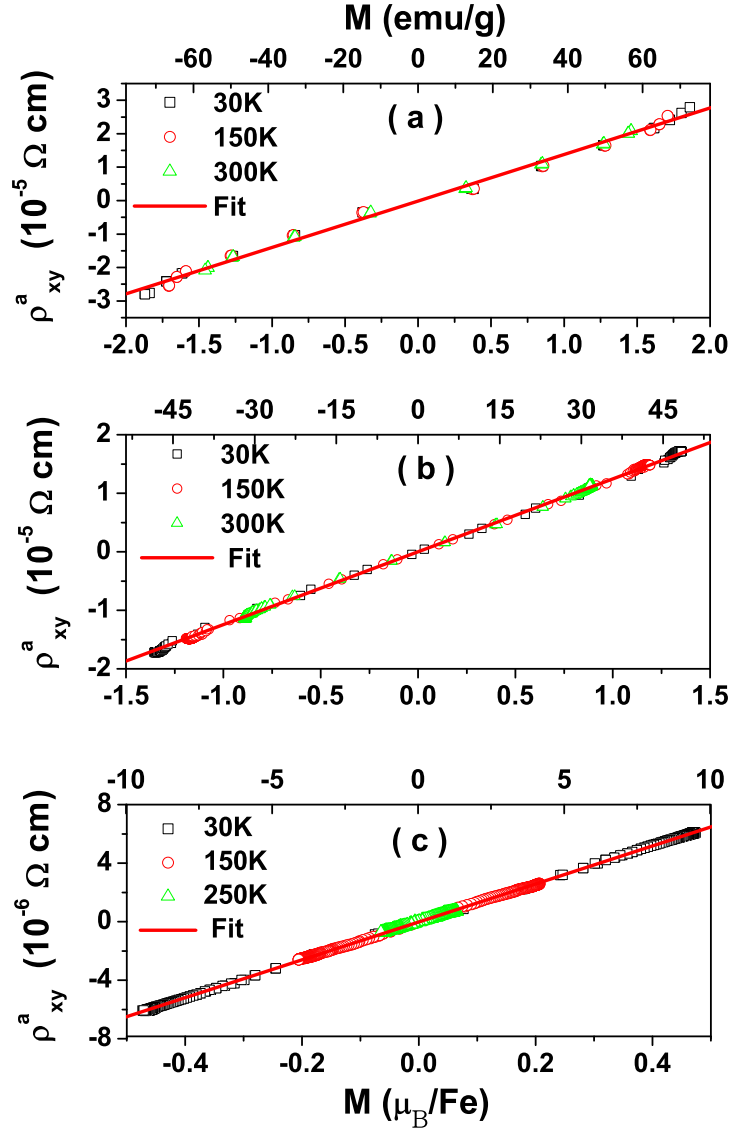
Fig. 6 Relation between ρ_{xy}^a and M, corresponding to all the data in Fig. 5 which were measured at different temperature and magnetic field. The solid line is the linear fitting, and the slope is the value of $R_S(H,T)$ for each sample. (a) $Fe_{0.5}Ge_{0.5}$, $R_S(H,T) = 3.57 \times 10^{-7} \ \Omega^{-1} \ cm^{-1} \ g^{-1} \ emu^{-1}$, (b) $Fe_{0.4}Ge_{0.6}$, $R_S(H,T) = 3.48 \times 10^{-7} \ \Omega^{-1} \ cm^{-1} \ g^{-1} \ emu^{-1}$, and (c) $Fe_{0.3}Ge_{0.7}$, $R_S(H,T) = 6.49 \times 10^{-7} \ \Omega^{-1} \ cm^{-1} \ g^{-1} \ emu^{-1}$.

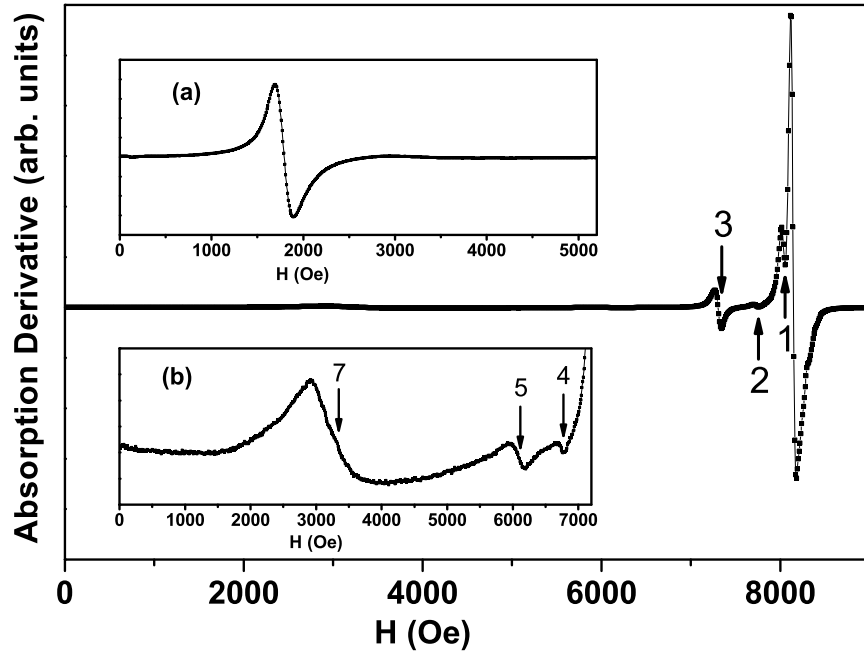**Fig. 7** The derivative spectra of the ferromagnetic resonance of the $Fe_{0.5}Ge_{0.5}$ thin film measured at room temperature for the applied magnetic field perpendicular to the film plane with the frequency of 9.77 GHz. Its low magnetic field region was enlarged to exhibit in the inset (b). The numbers 1, 2, 3, 4, 5, and 7 mark the spin-wave modes. The inset (a) is the ferromagnetic resonance when the applied magnetic field is in the film plane.